Deltares

WWQA
World Water Quality Alliance

Global Scenarios for Ecosystem Health

Global Scenarios for Ecosystem Health
Nutrient pollution and toxic stress

Authors
Joost van den Roovaart
Tineke Troost
Jos van Gils
Lex Bouwman (PBL, UU)
Arthur Beusen (PBL, UU)
Wilfred Altena
Hélène Boisgontier
Mark Hegnauer
Christian Liguori
Ira Wardani
Julia Bleser

Partners
Planbureau voor de Leefomgeving, 'S-GRAVENHAGE
Universiteit Utrecht, UTRECHT

Utrecht University

PBL Netherlands Environmental Assessment Agency

Global Scenarios for Ecosystem Health
Nutrient pollution and toxic stress

Client	United Nations Environment Programme
Contact	Dhr. Jian Lu, Director Science Division UNEP
Reference	Roovaart, J.C. van den, Troost, T., van Gils, J., Bouwman, A.F., Beusen, A.H.W., Altena, W., Boisgontier, H., Hegnauer, M., Liguori, C., Wardani, I., Bleser, J. (2022). Global Scenarios for Ecosystem Health. Deltares report 11207465-000-ZWS-0004
Keywords	World Water Quality Assessment, Nutrient pollution, Toxic stress, Global scenarios

Document control	
Version	0.1
Date	25-05-2022
Project nr.	11207465-000
Document ID	11207465-000-ZWS-0006
Pages	43
Classification	
Status	final

Author(s)		
Joost van den Roovaart	Deltares	
Tineke Troost	Deltares	
Jos van Gils	Deltares	
Lex Bouwman	PBL, UU	
Arthur Beusen	PBL, UU	
Wilfred Altena	Deltares	
Hélène Boisgontier	Deltares	
Mark Hegnauer	Deltares	
Christian Liguori	Deltares	
Ira Wardani	Deltares	
Julia Bleser	Deltares	

Summary

The Global Environment Monitoring Unit in the Science Division of the United Nations Environmental Programme (UNEP) provides support to the coordination of the World Water Quality Alliance (WWQA) by assessing key environmental issues and providing focused outlooks to strengthen science-based policy making. In this project, global scenarios of water quality were modelled for two indicators: nutrient pollution and toxic stress by Deltares in collaboration with the Netherlands Environmental Assessment Agency (PBL) and the University of Utrecht in the Netherlands (UU). The project is funded by UNEP and includes also in-kind contributions from the three partners.

Calculations of spatially explicit global scenarios of nutrient pollution (total nitrogen and total phosphorus) are based on the IMAGE model framework including the IMAGE-Global Nutrient Model (IMAGE-GNM) by PBL and UU, with consistent combinations of socioeconomic scenarios regarding population, economy, attitude towards sustainability and environment (socioeconomic pathways or SSPs) and climate (Representative Concentration Pathways or RCPs). Intermediate model results with respect to socio-economic drivers have been provided to Deltares as input to the scenario runs for toxic stress. The scenarios have been documented scientifically in a recent peer-reviewed publication (Beusen et al., 2022).
In all SSPs except SSP1, the inputs, delivery and export of N and P increase rapidly. The natural nutrient sources will continue to decline in all SSPs in future decades due to massive land use transformations, while agriculture, human sewage and aquaculture are becoming increasingly dominant (globally up to 80% of nutrient delivery). To achieve improved water quality, more efforts are needed than those employed in SSP1.

Global scenarios of toxic stress, consistent with the scenarios for nutrient pollution with respect to the used socioeconomic drivers and climate input were calculated by Deltares. Especially innovative is the method used to quantify toxic stress which calculates the cumulative impact of the full mixture of chemical substances, and which is expressed in terms of biodiversity loss using the indicator msPAF. This Toxic Stress indicator for the expected loss of aquatic species can be linked to the SDG Indicator 6.3.2 “Proportion of bodies of water with good ambient water quality”. We distinguish two different options for the calculations with the HIWAI indicator: a “best case” and a “worst case” calculation. For the “best case” option the percentage of land cover grid cells containing water bodies with a “good quality” (based on msPAF values <0.05, meaning less than 5% of species are expected to be lost) on a global scale in 2010 is 91% and shows a decrease in 2050 of 6% in the RCP6.0/SSP2 scenario and an even higher decrease of 8% in the more extreme RCP8.5/SSP5 scenario. For the “worst case” option the percentage of water bodies with a “good quality” on a global scale is much lower: 71% in the Baseline 2010 scenario and 62% in the RCP8.5/SSP5 scenario. The detailed calculation results will be made free available by the Deltares BlueEarth Digital Environment (https://blueearthdata.org/data).

Contents

	Summary	**4**
1	**Introduction**	**6**
1.1	Background	6
1.2	Previous work by Deltares, PBL and UU related to the WWQA	7
1.3	Objective of the project	7
2	**Nutrient pollution**	**9**
2.1	Introduction	9
2.2	Methods	9
2.2.1	Model used	9
2.2.2	Socioeconomic scenarios	10
2.2.3	Hydrology	11
2.2.4	Publication	11
2.2.5	Scenario data	11
2.3	Results	18
2.4	Conclusions	21
3	**Toxic stress**	**22**
3.1	Introduction	22
3.2	Methods	22
3.2.1	Hydrological modelling with Wflow	22
3.2.2	The HIWAI proxy – Modelling the effects of chemicals on aquatic species	23
3.2.3	Input parameters	28
3.2.4	Baseline and scenarios	28
3.3	Results	28
3.3.1	Geographical scale	28
3.3.2	Sustainable Development Goals	30
3.3.3	Baseline	30
3.3.4	Scenarios	30
3.4	Conclusions	36
4	**References**	**37**

1 Introduction

1.1 Background

United Nations Environment Assembly (UNEA) Resolution 3/10 on “Addressing water pollution to protect and restore water-related ecosystems” (UNEP/EA.3/Res.10) requested UNEP to develop a global water quality assessment in collaboration with UN-Water and relevant stakeholders by UNEA-5 (UNEP, 2018). During the Inception Meeting for the Assessment, around 50 organizations (UN, research, civil society, private sector), which had expressed interest to engage in the assessment, also expressed interest to work with UNEP in co-designing agendas and action around emerging issues. The group decided to form a World Water Quality Alliance (WWQA) as an open community of practice, representing a voluntary and flexible global Expert, Practitioners and Policy Network, which advocates the central role of freshwater quality in achieving prosperity and sustainability. It explores and communicates water quality risks in global, regional, national, and local contexts and points towards solutions for maintaining and restoring ecosystem and human health and wellbeing. It aims to serve countries throughout the lifetime of the 2030 Agenda for Sustainable Development (UN, 2015) and beyond.

As part of the delivery of this mandate from UNEA Resolution 3/10 and building upon the 2016 report *A Snapshot of the World’s Water Quality* (UNEP, 2016) and the resulting *Analytical Brief* (UN-Water, 2016), the WWQA will focus on generating and testing a data fusion approach combining different sources of water quality data contributing to the Assessment; horizon scanning, agenda setting and investigating selected priority topics to identify persistent or emerging water quality issues of key environmental and socio-economic concern; and co-designing and operationalizing water quality related services and products, based on a moderated in-country stakeholder driven process.

UNEP, and more specifically the Global Environment Monitoring Unit in the Science Division, provides support to the coordination of the Alliance through its WWQA Coordination Team. The work of the Alliance, specifically the World Water Quality Assessment, contributes to the implementation of the existing and upcoming UNEP Programme of Work (PoW) mainly under the Environment Under Review sub-programme project document ‘Assessing key environmental issues and providing focused outlooks to strengthen science-based policy making’. It is, however, in the heart of the Alliance that members are encouraged to collaborate on workstreams that cater as much for their own or other work programmes of members as well; this is to underline the co-benefit character of the Alliance.

The work plan of the World Water Quality Alliance consists of various thematic priority topics and related work streams. As a principle the workplan in its entirety reflects priorities and emerging issues identified for action by the Alliance in a peer exchange and prioritization process. Discussions and decisions on priorities of the work plan will take place during the annual global meeting (face to face or if required remotely). The work plan shall be a platform for all members to address water quality issues also within mandates and work programmes outside those of UNEA.

1.2 Previous work by Deltares, PBL and UU related to the WWQA

Together with other WWQA partners, Deltares has been working on water quality issues in close collaboration with the Netherlands Environmental Assessment Agency (PBL) and the University of Utrecht, the Netherlands (UU). Deltares shows its active membership of the WWQA by contributing to the global workshops (Inception Workshop 28-29 November 2018 Geneva, Global Workshop 16-20 September 2019 Ispra, 2nd Annual Global Meeting 27-28 January 2021 Virtual, 3rd Annual Global Meeting 26-27 January 2022 Virtual), organizing and hosting a WWQA workshop (Delft, the Netherlands, January 23-24 2020), by participating in the Technical Advisory Committee (TAC) of the WWQA, and as a member of the WWQA Task force and writing team for the *WWQA First Global Display of a Water Quality Baseline* (WWQA, 2021). Deltares coordinated the Ecosystem Health part of this document (Chapter 3.1), a focal topic of its internal Strategic Agenda 22-25, see Figure 1. 1 (Deltares, 2021).

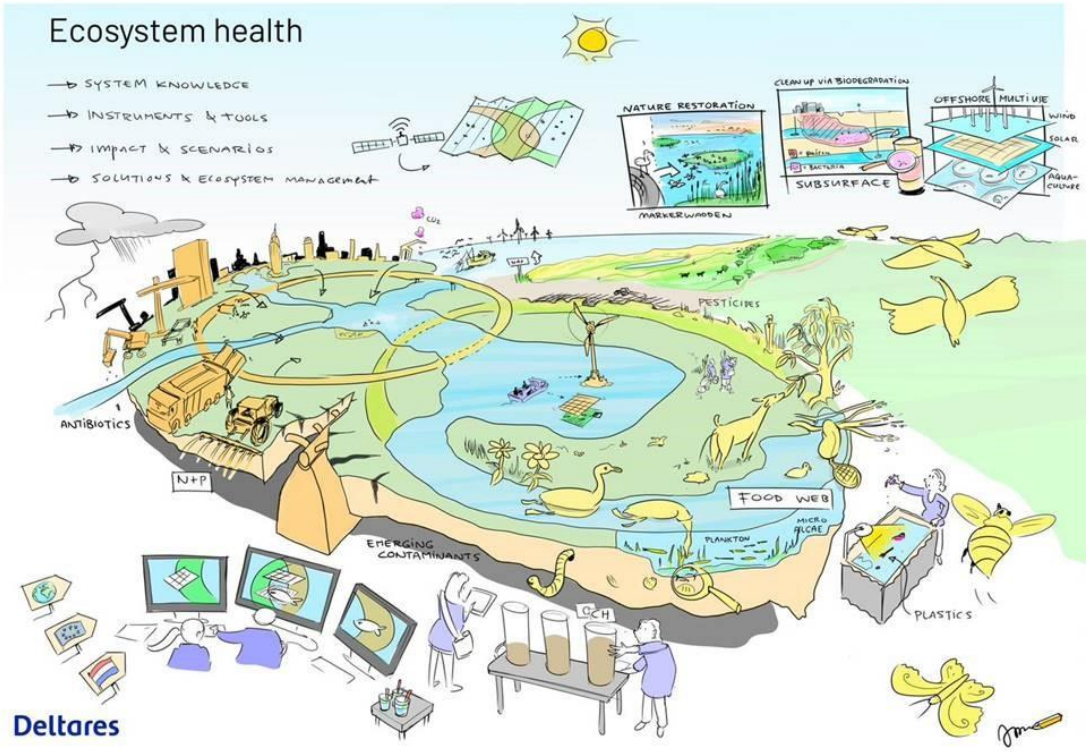

Figure 1. 1 Artist impression of the Deltares focus area Ecosystem Health.

Also, PBL and UU have been active within the WWQA work from the start. They have been contributed in the report *WWQA First Global Display of a Water Quality Baseline* (WWQA, 2021) and are engaged in several of the WWQA workstreams.

1.3 Objective of the project

The aim of this project is to establish global scenarios of water quality, zooming in on multiple drivers of change, their pressures, and impacts. The impacts are expressed in two indicators for ecosystem health: nutrient pollution and toxic stress. The project is funded through a Small-Scale Finding Agreement (SSFA) by UNEP. The project also includes in-kind contributions from the partners to generate the required models and model outcomes.

To ensure consistency with the work of the other partners in the WWQA, the definition of the scenario set-up has been aligned with the results of the closely related WWQA project “Scenario Analysis for World Water Quality Assessment” from Wageningen University (WUR). The outcome of the first WUR-workshop (June 2021) is also the basis for the global scenarios for nutrient pollution and toxic stress.

The first deliverable under Activity 1 is a set of spatially explicit global scenarios of nutrient pollution (total nitrogen and total phosphorus). Calculations will be based on the IMAGE model by PBL and UU, with consistent combinations of socioeconomic scenarios (population, economy, attitude towards sustainability and environment) and climate. Intermediate model results with respect to socio-economic drivers have been provided to Deltares as input to the scenario runs for toxic stress.

The second deliverable is a set of spatially explicit global scenarios of toxic stress, consistent with the scenarios for nutrient pollution with respect to the used socioeconomic drivers and climate input. Calculations are based on Wflow D-Emissions model by Deltares, which has been run for the baseline year 2015 only for the African continent and have been described in the *WWQA First Global Display* (WWQA, 2021). In this SSFA project, these calculations are upscaled to a global coverage and extended with scenario calculations for 2050, compared to the baseline year 2010. Especially innovative is the method used to quantify toxic stress which calculates the cumulative impact of the full mixture of chemical substances, and which is expressed in terms of biodiversity loss.

2 Nutrient pollution

2.1 Introduction

Citation from *WWQA First Global Display of a Water Quality Baseline* (WWQA, 2021):

> Fertilizers, primarily nitrogen (N) and phosphorus (P) that have played a major role in the increased food production, enter soils, groundwater and surface water and are transported towards coastal seas. This has resulted in a wide range of environmental problems, ranging from groundwater pollution, loss of habitat and biodiversity, the creation of coastal dead zones, occurrence of harmful algal blooms, and fish kills as well as human health impacts (Damania et al. 2019, Diaz and Rosenberg 2008; Howarth et al. 2011; Michalak et al. 2013; Rabalais et al. 2001; Turner et al. 2003; Vollenweider 1992).

2.2 Methods

2.2.1 Model used

To project future riverine nutrient pollution, it is important to base projections on scenarios generated by integrated assessment models and align them with earth system models. In this study we use the implementation of the shared socioeconomic pathways (SSPs) with the model framework Integrated Model to Assess the Global Environment (IMAGE) (Stehfest et al., 2014), with land-use trends specifically described in Doelman et al. (2018). Here we use an updated version of this implementation, using the same scenario assumptions and resulting in similar projections for domestic production and trade of energy, food, feed and biofuel crops, meat and milk, land use and cover projections, greenhouse gas emissions and climate change (IMAGE version 3.2; see https://eartharxiv.org/repository/view/2759/; and see Table 2. 6). The base year is 2015, except for the hydrology where SSP2 is used for 2011-2015. However, all SSPs have the same trajectories for land use between 2015 and 2020 based on SSP2 and from 2021 onwards the scenarios begin to deviate. The scenarios have been described in detail in a recent peer-reviewed publication (Beusen et al., 2022).

For generating projections of nutrient pollution of water bodies, the IMAGE model framework includes thethe IMAGE-Global Nutrient Model (IMAGE-GNM; (Beusen et al., 2015). IMAGE-GNM is a global, spatially explicit, distributed model that couples IMAGE with the global hydrological model PCR-GLOBWB (Van Beek et al., 2011; Sutanudjaja et al., 2018) as the basis for describing flow and retention/removal of N and P delivery from soils to surface waters. IMAGE-GNM can study the impact of multiple environmental changes over prolonged time periods. IMAGE-GNM uses the nutrient spiralling approach to describe in-stream retention of both N and P with a yearly time step (following Wollheim et al. (2008) (Newbold et al., 1981).). A detailed description of IMAGE-GNM is given in Beusen et al. (2015), with additional validations provided in Supplementary Materials.

The data flows in IMAGE-GNM including PCR-GLOBWB are presented in Figure 2. 1. Spatial land cover distributions for the 20th century are from HYDE and IMAGE (1970 onwards) (Klein Goldewijk et al., 2010). Global climate data are used in PCR-GLOBWB for computing the water balance, runoff, and discharge for each year. Global climate data are used in PCR-GLOBWB for computing the water balance, runoff and discharge for each year. For each grid cell, IMAGE-GNM provides the delivery of N and P to the surface water via diffuse sources (agriculture, natural ecosystems, aquaculture) and point sources (wastewater) (Figure 2. 1). Soil nutrient budgets (the difference between inputs and outputs) are calculated for each grid cell. Nitrogen inputs considered are fertilizer, animal manure, atmospheric deposition and biological N fixation. Phosphorus inputs are fertilizer and animal manure.

Nutrient outputs are withdrawal by agricultural crops in harvested parts and by grazing or mowing of grass and ammonia volatilization. Natural ecosystems are assumed to be mature (i.e. net withdrawal is zero), except for vegetation in floodplains where part of the litter is transported by the water.

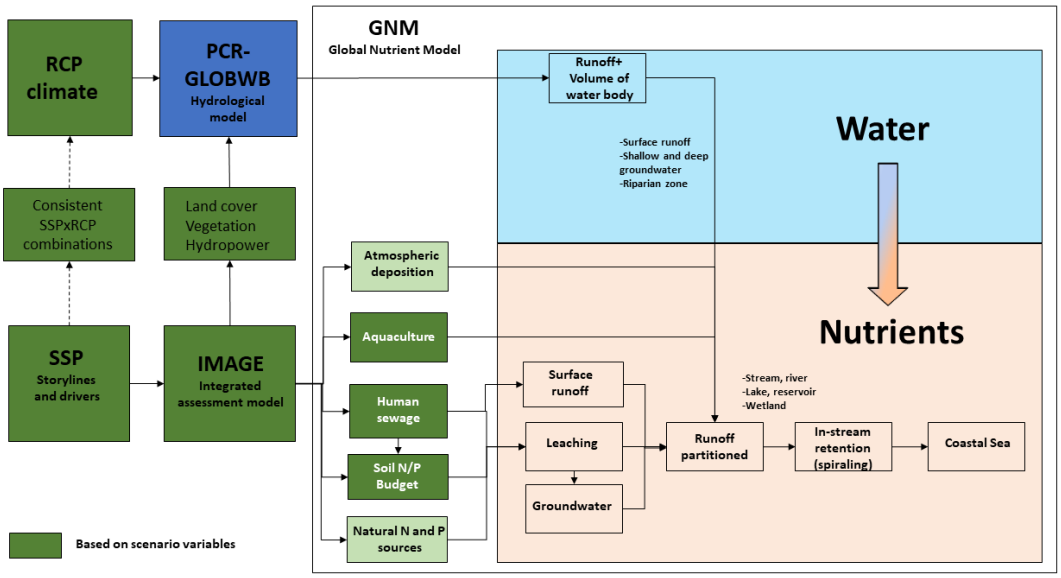

Figure 2. 1 Scheme of the model computations of nutrient pollution of global water bodies according to the SSP scenarios with the IMAGE-Global Nutrient Model (GNM).

Each grid cell receives water containing N and P from upstream grid cells, and from diffuse and point sources within the grid cell. After accounting for in-stream retention, water and nutrients are transported to downstream grid cells. Discharge is routed to obtain the accumulated water and nutrient flux in each grid cell, through rivers, lakes, wetlands, and reservoirs (Figure 2. 1). The model accounts for the "memory" of groundwater, where travel times may amount to several decades. Cumulative N storage in deep groundwater between 1900 and 2000 amounted to around 376 Tg (Bouwman et al., 2013). The retardation due to this cumulative reservoir varies considerably depending on the history of fertilizer use and manure management, as well as the geohydrological situation and climate (Van Drecht et al., 2003). In addition, the soil component has a memory, which is the change in soil P content due to accumulation in grid cells with a surplus, or loss due to surface runoff.
In this report, we show IMAGE-GNM data covering the time period 1970-2050.

2.2.2 Socioeconomic scenarios

IMAGE-GNM has been used to integrate societal and technological processes and their impact on the change of pools of nutrients in landscapes and impacts on nutrient water quality for the 20th century (Beusen et al., 2016). Global riverine nutrient delivery to inland waters and export to the coastal zone in the coming century will strongly depend on global (economic) development and we will therefore follow the community consensus: the five shared socioeconomic pathways (SSPs) (O'Neill et al., 2014; van Vuuren et al., 2014). A sustainability scenario (SSP1) in which we make good progress toward sustainability, with ongoing efforts to achieve development goals while reducing resource intensity and fossil fuel dependency. A middle of the road pathway (SSP2) or business-as-usual world, a fragmented world with regions differing widely in economic development (SSP3), a scenario with a highly unequal world in which a relatively small, rich global elite is responsible for most of the greenhouse gas emissions, while a larger, poor group that is vulnerable to the impact of climate changes, contributes little to the harmful emissions (SSP4) and SSP5 involving traditional development with a focus on economic growth with continued high greenhouse gas emissions.

Regarding the basic socio-economic scenarios (Table 2. 6), it is clear that population growth is particularly rapid in SSP3 in BRIC and developing countries, while population growth is modest in the sustainability SSP1 and the fossil-fuel based SSP5 scenarios. This is related to the economic growth, which is most rapid in SSP5 and much slower in SSP3 than in all other scenarios. Livestock production is expanding rapidly in SSP5 (related to high income growth), and much less in SSP1 than in the other scenarios.

The scenario components wastewater and agricultural nutrient management follow the SSP storylines and have been quantified in line with the assumptions made for all other aspects (energy, land use, sustainability, attitude towards environmental problems, etc., see Table 2. 6), as described in detail elsewhere (Van Puijenbroek et al., 2019).

Regarding nutrient use efficiency, SSP1 shows most progress towards high-efficiency and low-pollution agriculture, and at the same time there is a large effort to connect inhabitants to sewage systems and wastewater treatment facilities. In SSP2, SSP3 and SSP4, there is no change in agricultural efficiency, and connection to sewage systems and wastewater treatment follows current trends or is slowly advancing, meaning that with fast population growth, the excreta, and detergent emissions from large parts of the population is not treated in the coming decades.

2.2.3 Hydrology

The socio-economic projections lead to different scenarios for greenhouse gas emissions, climate change and radiative forcing. For example, there is a relatively low forcing level (but not low enough to achieve 2.6 W m^{-2}) in the sustainable development SSP1 scenario and a high forcing level in the fossil-fueled rapid growth SSP5 scenario. Therefore, each SSP has been combined with one of the pre-defined Representative Concentration Pathways (RCPs, see van Vuuren et al. (2014)) from the HadCM3 Global Circulation Model (MetOffice, 2020). These climate runs were bias-corrected with observed weather data over the historical period 1960-1999 (Hempel et al., 2013). The global average radiative forcing values in the year 2100 in the RCPs (RCP2.6, RCP4.5, RCP6, and RCP8.5 leading to 2.6, 4.5, 6.0, and 8.5 W m^{-2}, respectively) match the forcing levels according to the SSPs (van Vuuren et al., 2017) (Figure 2. 1). In the IMAGE framework, this yields the combinations SSP1-RCP4.5, SSP2-RCP6.0, SSP3-RCP6.0, SSP4-RCP6.0 and SSP5-RCP8.5. The PCR-GLOBWB hydrology model was run up till the year 2099 using these RCP simulations (Figure 2. 1). Here, data for the period up till 2050 were used.

2.2.4 Publication

The scenarios have been documented scientifically in a recent peer-reviewed publication (Beusen et al., 2022).

2.2.5 Scenario data

In this project, the spatially explicit scenario output from IMAGE-GNM was organized in Network Common Data Form (Netcdf), i.e., a self-describing, machine-independent data format that support the creation, access, and sharing of scientific data. All parameters in the netCDF files have a spatial resolution of 0.5 X 0.5 degree. There are 360 rows and 720 columns in each dataset. The global extent of the grids is longitude between -180 and 180 degrees and latitude between -90 and 90. The time period for all datasets is 1970 – 2070. The scenario assumptions start after 2015 (except for the hydrology, which is based on SSP2 for 2011-2015). The results are reported every five years. The projection of all the datasets is WSG84 (global lat-lon projection). Data is available on:
https://dataportaal.pbl.nl/downloads/IMAGE/GNM/

The data consist of 8 Netcdf files for each scenario. Filenames consist of the prefix Output-IMAGE_GNM-<scenarioname>_oct2020-, followed by:

1 LandCover-v2 (Table 2. 1)
2 Nitrogen_CroplandBudget-v2 (Table 2. 2)
3 Nitrogen_NonAgriculturalLandBudget-v2 (Table 2. 2)
4 Nitrogen_PastureBudget-v2 (Table 2. 2)
5 Phosphate_CroplandBudget-v2 (Table 2. 3)
6 Phosphate_PastureBudget-v2 (Table 2. 3)
7 Nitrogen_Rivers-v2 (Table 2. 4)
8 Phosphorus_Rivers-v2 (Table 2. 5)

Table 2. 1. Data of the (1) land cover.

Total	Mha	Total land area excluding urban area. So total land is not constant in time.
Cropland	Mha	Total cropland area
Pasture	Mha	Total pasture area
NonAgriculturalLand	Mha	Total area of land under natural vegetation

Table 2. 2. Data of the (2)-(4) Nitrogen budgets for (2) Cropland; (3) Land under natural vegetation; (4) Pastureland.

AtmosphericDeposition	MtN	Total nitrogen deposition on cropland
BiologicalFixation	MtN	Biological nitrogen fixation on cropland
Fertilizer	MtN	Total fertilizer use on cropland, including recycling from waste water
Manure	MtN	Manure recycled from confinement (and grazing in the case of pastureland)
Withdrawals	MtN	N in harvested parts
HarvestedCrops	MtN	N in harvested parts
NutrientSurplus	MtN	Difference between cropland inputs and crop production minus NH3 volatilization
N2	MtN	N2 emission from denitrification from soil on cropland
Ammonia volatilization	MtN	NH3 emission from soil on cropland
N2O	MtN	N2O emission from soil on cropland
NO2	MtN	NOx emission from soil on cropland
NO3	MtN	Nitrogen leaching to groundwater

Table 2. 3. Data of the (5)-(6) Phosphate (P2O5) budget for (5) Cropland; (6) Pastureland.[a]

Fertilizer	Mt P2O5	Total fertilizer use on cropland, including recycling from waste water
Manure	Mt P2O5	Manure recycled from confinement (and grazing in case of pastureland)
Withdrawals	Mt P2O5	P2O5 in harvested parts
HarvestedCrops	Mt P2O5	P2O5 in harvested parts
NutrientSurplus	Mt P2O5	Difference between cropland inputs and crop production

[a] P budgets for land under natural vegetation are not available; P inputs consist of weathering, which is included in P delivery and transport in rivers.

Table 2. 4. Data for the (7) nitrogen delivery and transport in rivers.

Nsurface_runoff_nat	Kg N/year	N load from surface runoff from land under natural vegetation
Nsurface_runoff_agri	Kg N/year	N load from surface runoff from agricultural land
Ngroundwater_nat	Kg N/year	N load from groundwater from land under natural vegetation
Ngroundwater_agri	Kg N/year	N load from groundwater from agricultural land
Nvegetation	Kg N/year	Nitrogen load in litter from terrestrial vegetation in flooded areas
Ndeposition_water	Kg N/year	Direct nitrogen deposition on water
Naquaculture	Kg N/year	Nitrogen load from aquaculture to surface water
Nsewage	Kg N/year	Nitrogen load from waste water (household and industry) to surface water
Nloss_channel	Kg N/year	Nitrogen retention in water column in main channel
Nloss_streams	Kg N/year	Nitrogen retention in small streams (orders <6) before reaching main channel
Nload	Kg N/year	Accumulated nitrogen load from all sources in the river accounting for in-stream retention and inflow from upstream grid cells (Nload = outflow from each grid cell)
Nconc	mg N L^{-1}	Nitrogen concentration in main channel
Sgd	Kg N/year	Nitrogen in submarine groundwater discharge to coastal sea

Table 2. 5. Data for the (8) phosphorus delivery and transport in rivers.

Discharge	Km^3	Discharge of river
Psurface_runoff_nat	Kg P/year	P load from surface runoff from land under natural vegetation
Psurface_runoff_agri	Kg P/year	P load from surface runoff from agricultural land
Pweathering	Kg P/year	Phosphorus load from weathering reaching surface water
Pvegetation	Kg P/year	Phosphorus load in litter from terrestrial vegetation in flooded areas
Paquaculture	Kg P/year	Phosphorus load from aquaculture to surface water
Psewage	Kg P/year	Phosphorus load from waste water (household and industry) to surface water
Ploss_channel	Kg P/year	Phosphorus retention in water column in main channel
Ploss_streams	Kg P/year	Phosphorus retention in small streams (orders <6) before reaching main channel
Pload	Kg P/year	Accumulated phosphorus load from all sources in the river accounting for in-stream retention and inflow from upstream grid cells (Nload = outflow from each grid cell)
Pconc	mg P L^{-1}	Phosphorus concentration in main channel

Table 2. 6 General characteristics of the shared socioeconomic pathways (SSP) and corresponding IMAGE results for general agricultural production and land use data.

	Region*	1970	2015	2050				
				SSP1	SSP2	SSP3	SSP4	SSP5
Keyword				Sustainability	Middle of the Road	Fragmentation	Inequality	Conventional development
Technological development				Rapid	Medium	Slow	Slow	Rapid
Progress towards development goals				Good	Some	Failure to achieve goals	Highly unequal	Market-driven
Resource intensity				Low	Medium	Little progress	Highly unequal	Conventional (fossil fuel)
Attitude towards environmental problems				Proactive	Indifferent	Reactive	Reactive	Reactive
Sewage connection				Strong increase	Current trend	Slow	Slow	Strong increase
Wastewater treatment efficiency				High	Current trend	Medium	Medium	High
Meat consumption				Low	Medium	Unequal	Unequal	High
Agricultural nutrient use efficiency				High	No change	Low	Low	High, but also exploding food production
Population (million inhabitants)	World	3776	7382	8744	9349	10034	9308	8825
	Industrialized	828	1055	1200	1174	1015	1114	1338
	BRIC	1673	3107	3248	3454	3715	3235	3251
	Rest of world	1274	3221	4297	4721	5304	4959	4236

	Region*	1970	2015	2050				
GDP/capita (US$/yr)	World	4263	7879	22463	16701	11501	16065	28603
	Industrialized	15998	35310	60864	56000	51769	62548	70266
	BRIC	621	3629	21915	14631	9200	14694	27949
	Rest of world	1419	2992	12156	8445	5405	6518	15945
GHG emissions (Pg C-eq/yr)	Global	6	14.0	16.1	20.3	19.6	15.7	32.2
Global mean temperature increase (℃)**	World	0.2	1.1	2.2	2.3	2.3	2.2	2.6
Meat production (Mton/yr)	World	118	397	516	592	618	559	744
	Industrialized	68	122	108	142	144	136	190
	BRIC	24	169	239	251	256	237	320
	Rest of world	26	105	170	199	218	186	235
Crop production (Mton dm/yr)	World	1751	4567	6258	6664	6792	6311	7253
	Industrialized	615	1109	1222	1357	1341	1325	1488
	BRIC	593	1859	2343	2389	2442	2309	2550
	Rest of world	544	1599	2693	2917	3009	2676	3214
Area arable and permanent crops (Mha)	World	1410	1596	1623	1834	1961	1787	1887
	Industrialized	443	383	357	388	387	364	383
	BRIC	446	516	472	510	530	487	518
	Rest of world	522	697	794	936	1045	936	985
Average crop yield (Mg dry matter/ha/yr)	World	1.2	2.9	3.9	3.6	3.5	3.5	3.8

	Region*	1970	2015	2050				
	Industrialized	1.4	2.9	3.4	3.5	3.5	3.6	3.9
	BRIC	1.3	3.6	5.0	4.7	4.6	4.7	4.9
	Rest of world	1.0	2.3	3.4	3.1	2.9	2.9	3.3
Total agricultural area (Mha)	World	4476	4822	4592	5271	5470	5145	5460
	Industrialized	1195	1080	972	1081	1082	1027	1098
	BRIC	1102	1314	1191	1383	1439	1345	1448
	Rest of world	2179	2428	2429	2806	2949	2773	2913
Biofuel area (Mha)	World	0	6	44	51	0	0	58
Biofuel area (% of cropland)	World	0	1	11	12	0	0	13

2.3 Results

The five SSP scenarios present a diverse set of possible futures, with different basic population and economic pathways, and varying assumptions with regard to the attitude towards the environment and people's approaches to solve environmental pollution, ranging from reactive to proactive. Despite this wide spectrum of futures, the outcomes with regard to water quality show striking similarities.

Exploring the changes during 1970-2015 and 2015-2050 according to the five SSPs shows that the natural nutrient sources have been declining in the past decades and will continue to decline in all SSPs in future decades due to massive land use transformations, while agriculture, human sewage and aquaculture are becoming increasingly dominant (globally up to 80% of nutrient delivery). Figure 2. 2 shows the result of IMAGE-GNM for N concentrations in surface water for 2015, and for 2050 for the five SSP scenarios.

In all SSPs except SSP1, the inputs, delivery and export of N and P increase rapidly. It is difficult to decelerate the nutrient cycles, because even in the sustainable SSP1 scenario the reduced growth of agricultural production with higher efficiency, and rapidly growing access to improved sanitation, do not lead to a reduction of total N and P river export. To achieve improved water quality, more efforts are needed than those employed in SSP1. Water quality improvement may be achieved through reduction of consumption of livestock products, fine-tuning and closing nutrient cycles in agriculture with integration of crop and livestock production systems, improved management to increase agricultural nutrient use efficiencies, and advanced wastewater treatment to replace primary and secondary installations.

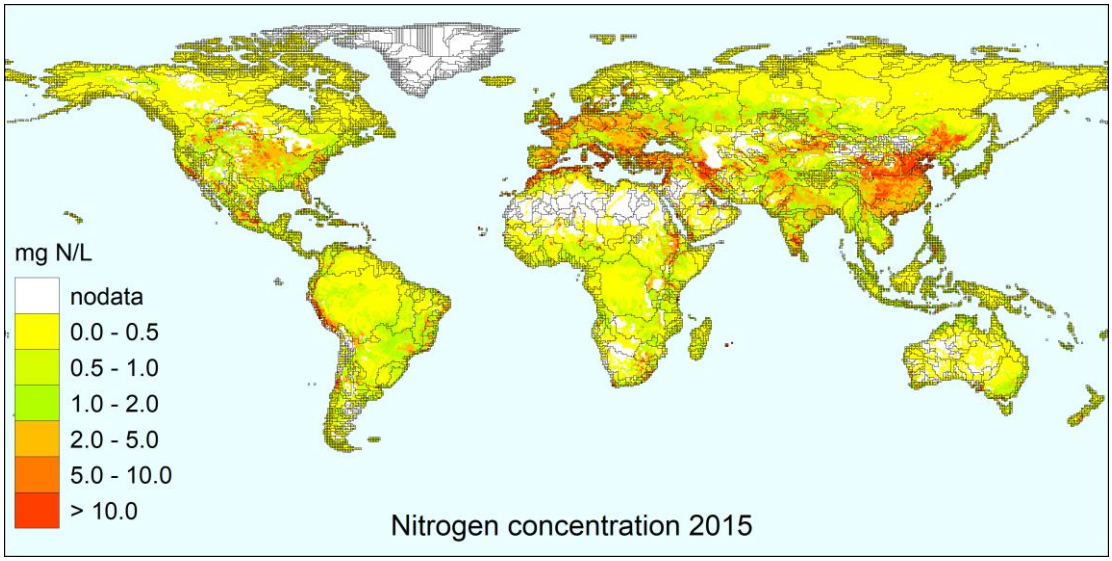
mg N/L
nodata
0.0 - 0.5
0.5 - 1.0
1.0 - 2.0
2.0 - 5.0
5.0 - 10.0
> 10.0
Nitrogen concentration 2015

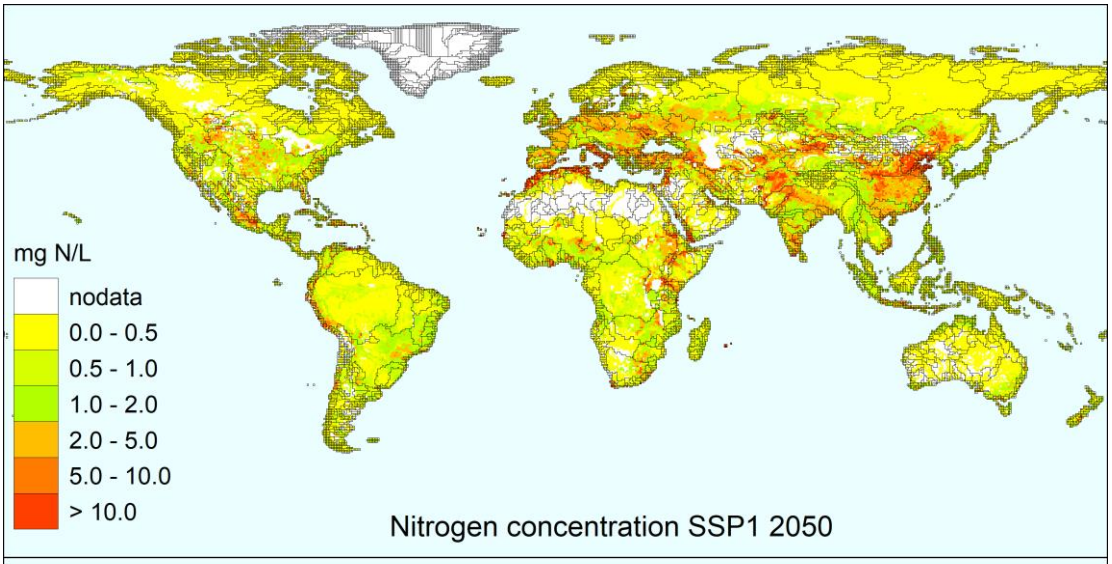
mg N/L
nodata
0.0 - 0.5
0.5 - 1.0
1.0 - 2.0
2.0 - 5.0
5.0 - 10.0
> 10.0
Nitrogen concentration SSP1 2050

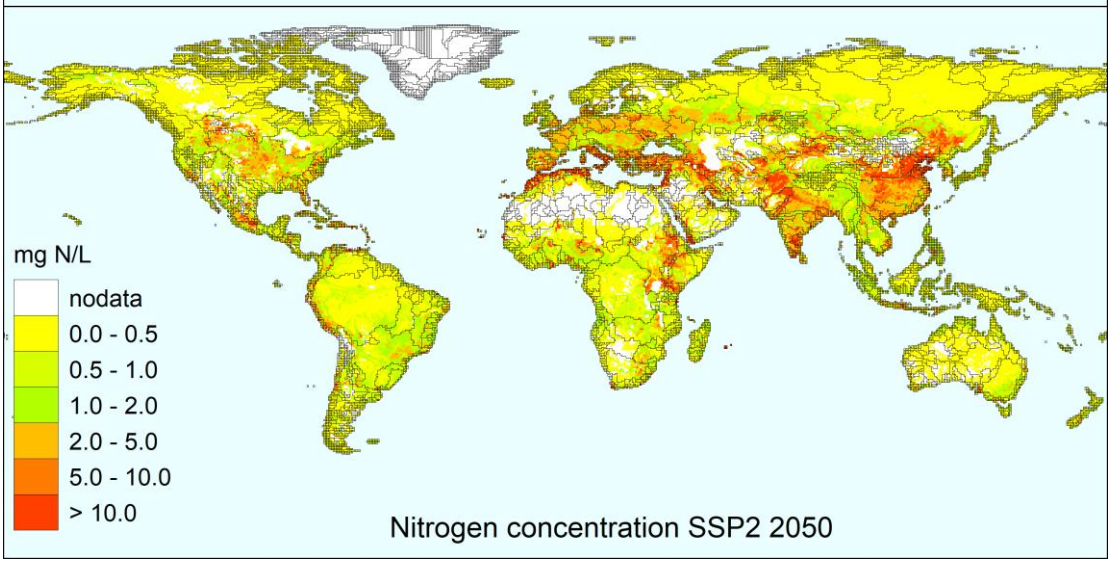
mg N/L
nodata
0.0 - 0.5
0.5 - 1.0
1.0 - 2.0
2.0 - 5.0
5.0 - 10.0
> 10.0
Nitrogen concentration SSP2 2050

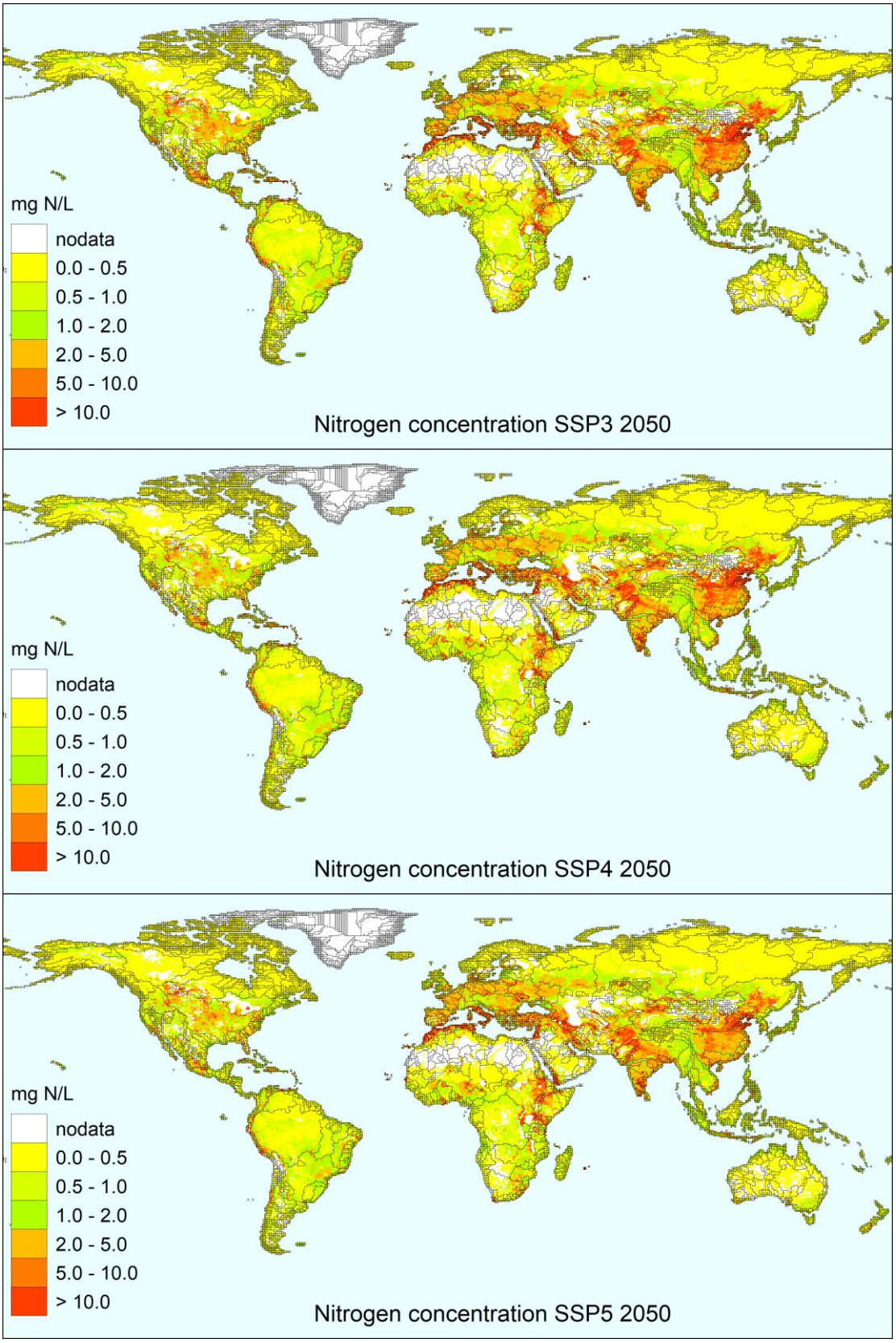

Figure 2. 2 N concentrations in mg N L^{-1} in surface water for 2015, and for 2050 for the five SSP scenarios.

2.4 Conclusions

Based on the calculations of the nutrient pollution scenarios, the following conclusions can be made:

- The SSP scenarios vary in assumptions regarding population data and economic pathways but show strong similarities in their outcomes. Especially, the increasing input, delivery and export of N and P is seen in every scenario.
- Changes during 1970-2015 and 2015-2050 indicate a decline of natural nutrient sources in the past decades that will continue in the future due to massive land transformations.
- Agriculture, human sewage and aquaculture will increase as a source for nutrient input (globally op to 80%).
- To improve water quality in the future, even more efforts are needed than included in the SSP1 scenario, e.g. reduction of consumption of livestock products, fine-tuning and closing nutrient cycles in agriculture with integration of crop and livestock production systems, improved management to increase agricultural nutrient use efficiencies, and advanced wastewater treatment to replace primary and secondary installations.

3 Toxic stress

3.1 Introduction

Citation from *WWQA First Global Display of a Water Quality Baseline* (WWQA, 2021):

> Currently, over 350,000 chemicals and mixtures of chemicals have been registered for production and use (Wang et al. 2020). And, as a result of their use, many of these chemicals find their way to freshwater systems (Stroomberg et al. 2018, Liška et al. 2015, Schulze et al. 2019) and coastal waters (UNESCO and HELCOM 2017). There they may accumulate and negatively affect the aquatic ecosystem.

3.2 Methods

3.2.1 Hydrological modelling with Wflow

The fate and transport of pollutants through the landscape is highly dependent on water movements. In most cases, pollutants are emitted on land, leach into the soil or are picked up by water during rain events, and subsequently transported towards and into the rivers. To model water quality, it is essential to first understand and assess the hydrology of the catchment or region of interests.

For this purpose, we used Wflow, a hydrological modelling platform that allows users to account for precipitation, interception, snow accumulation and melt, evapotranspiration, soil water, surface water and groundwater recharge in a fully distributed environment. Wflow has been successfully applied worldwide for analysing flood hazards, drought, climate change impacts and land use changes, and is growing to be a world leader in hydrology solutions. It includes a number of hydrological modules such as the SBM (Simple Bucket Model), HBV (Hydrologiska Byråns Vattenbalansavdelning), other surface water generation concepts, water routing modules such as the kinematic wave or Darcy for groundwater flow.

In this project, the physical-based SBM concept was chosen (Figure 3. 1) as it is targeted to perform hydrological simulations using GIS raster data based on global datasets, which makes it the concept of choice in data scarce environments and for global studies.

Based on gridded topography, soil, land use and climate data, Wflow-SBM calculates all hydrological fluxes at any given point in the model at a given time step. The movement of surface water across the landscape is determined by the reservoir and kinematic wave modules providing an accurate representation of river discharges.

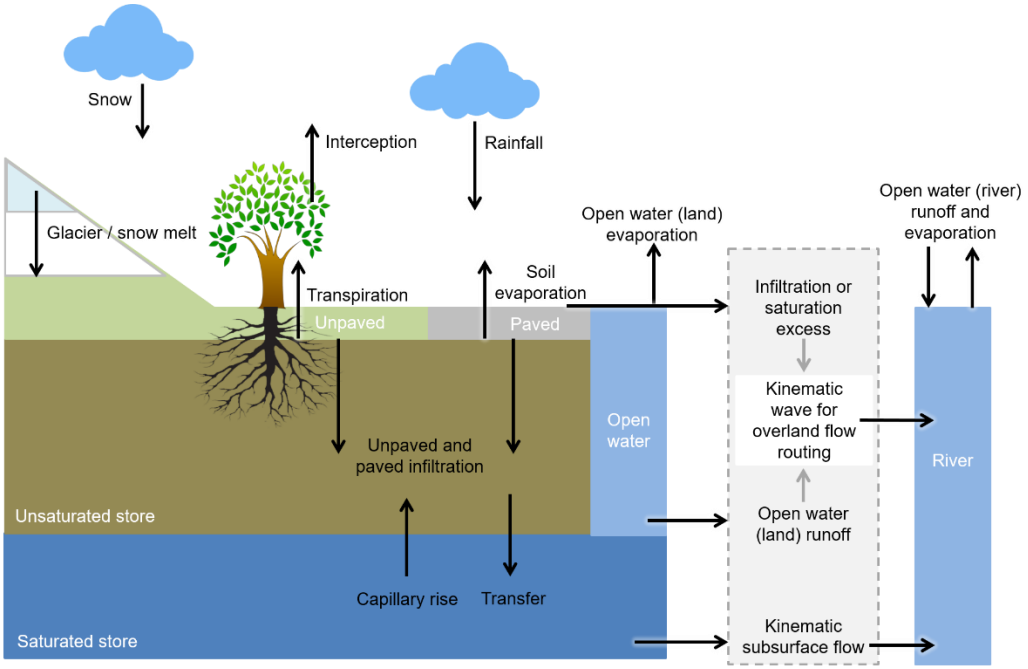

Figure 3. 1 Overview of the main hydrological processes in the Wflow SBM cell.

3.2.2 The HIWAI proxy – Modelling the effects of chemicals on aquatic species

Why a proxy-based method?

Water quality modelling is an accepted tool to supplement surface water quality monitoring data for water quality assessments. It has the advantage of providing numeric concentration values of simulated substances in all points of the model domain at all times during the simulated period. Thus, modelling avoids the weaknesses of water quality monitoring data, being the limited spatial and temporal coverage and the analytical complexities of measuring low concentrations (limits of detection and quantification). Brack et al. (2017) provide a discussion on this subject in a European water management context. In addition, model-based approaches offer strong diagnostic capabilities (gain system understanding, identifying knowledge and data gaps) and offer prognostic capabilities (scenarios). These diagnostic and prognostic capabilities provide understanding of cause-effect relations, which is a prerequisite for effective prevention and/or mitigation of water quality issues. The disadvantage of model-based approaches is that their accuracy is generally considered lower than that of water quality monitoring, despite modellers' efforts to carefully set up, calibrate and validate their models.

Traditionally, water quality modelling consists of three different steps:

1 the compilation of a pollution load inventory;
2 the set-up of a water quality model coupled to a hydrodynamic or hydrology model, including bio-geochemical processes formulations suited for the water quality variables to be studied;
3 the calibration of some parameters in the biogeochemical processes formulations by the comparison of simulation results to field data.

For the issue of toxic stress stemming from the occurrence of chemicals in surface water, the traditional water quality modelling approach presents difficulties. The number of man-made chemicals entering the market is increasing rapidly. Over 350,000 chemicals and mixtures of chemicals have been registered for production and use (Wang et al., 2020). Numerous references witness that thousands of individual chemicals have been detected in surface waters, while non-target analyses of surface waters reveal the presence of many more. Traditional water quality modelling requires the availability of data and understanding to conduct the steps listed above. For many emerging "data-poor" chemicals this requirement is not satisfied. Moreover, the sheer substances count makes substance-by-substance water quality modelling virtually impossible.

The proxy-based approach as outlined in this section aims to avoid the complexities listed above, while still providing a useful water quality modelling approach for the assessments under consideration.

The HIWAI proxy

For the present assessment the "Human Impact and Water Availability Indicator" (HIWAI) proxy was used. This concept arose from an EU funded research project called SOLUTIONS conducted by a large European consortium in 2013-2018. In this project, emission, fate & transport and effects models were developed suitable to larger groups of "data poor" chemicals (van Gils et al. 2019; 2020). The project's ambition to simulate a realistic mixture of chemicals rather than just a few individual chemicals, materialized in a Europe wide assessment of simulated mixture effects on aquatic species assemblages of 1,785 chemicals (Posthuma et al. 2019).

The HIWAI proxy is based on the time- and space-dependent simulated concentration of a conservative tracer. The simulation uses an open-source transport model (Deltares, 2022) coupled to the hydrology model discussed above. In the work by van Gils et al. (2020), emission modelling was driven by data on the EU-wide use volume of chemicals as registered under the REACH legislative framework (ECHA, 2022). The emissions were downscaled using the following quantity ("pressure proxy" or PP):

$$PP = pop \times pcGDP \times (1-PCD * PCL)$$

where *pop* is the population number, *pcGDP* is the per capita GDP, *PCD* is the degree of environmental management and control applied (0 = no control; 1 = maximum control) and *PCL* is the reduction of chemicals releases achieved at maximum control.

The definition of *PP* for downscaling chemicals emissions was based on certain assumptions. The consumption of chemicals by society is assumed proportional to its GDP. This assumption can be supported by the comparability of the increase of the global chemicals production volume and the global GDP. Between 1989 and 2018, the average global chemicals production volume increased by 3.1%/year (based on information from the American Chemistry Council (2019)), while the global GDP in that period increased by an average 2.9%/year (World Bank, 2022). The *PCD* could be expressed as a function of the per capita GDP: *PCD* increases linearly from 0 to 1 while the per capita GDP increases from 0 to 40 k$/a and stays at 1 where the per capita GDP exceeds 40 k$/a. The shape of this relation and the breakpoint at per capita GDP = 40 k$ can be recognized in a correlation to per capita GDP of Urban Waste Water Collection and Treatment infrastructure in European countries (van Gils et al. 2020) and in statistic data for leakages of plastic waste (Lebreton et al., 2019). The factor *PCL* was calibrated by van Gils et al (2020) to a value of 0.5 (meaning that full environmental management and control applied leads to 50% lower chemicals emissions).

For the simulation of the HIWAI indicator, a conservative tracer is emitted in the surface water network in proportion to *PP*. The HIWAI indicator is then obtained by calculating the mean concentration of the tracer.

The relation between the HIWAI proxy and the effects of chemicals on aquatic species

As mentioned above, mixture effects on aquatic species assemblages of 1,785 chemicals were calculated by Posthuma et al. (2019), using simulated concentrations of these chemicals by van Gils et al. (2020). They argue that this simulated spatial field of effects on aquatic species is a realistic and credible metric of toxic stress. Posthuma et al. (2019) use the so-called msPAF method to quantify toxic stress. The method uses species sensitivity distributions (SSD) characterized by the median (μ) and the variability (σ) of the log-normal across-species toxicity data distribution for each chemical (De Zwart and Posthuma, 2006). The intersection of a representative concentration value with this SSD for an individual chemical provides the Potentially Affected Fraction of species (PAF), a metric that varies between 0 and 1 (no to all species affected). A subsequent mixture modelling step quantifies the multi-substance PAF (msPAF) to provide a single number between 0 and 1 expressing the estimated fraction of aquatic species affected by the mixture. The method can be driven by different types of toxicity data. When using SSDs for the chronic NOEC endpoint, an estimate is obtained of initial effects or distress to sensitive species. When using SSDs for the acute EC50 endpoint, an estimate is obtained of species loss. The selection of a representative concentration value should match the selected endpoint: for the estimation of chronic effects a 50%tile (P50) is suitable, while for the estimation of acute effects due to a peak exposure a 99%tile (P99) is used.

Posthuma et al. (2019) discuss various examples of applications of this method that demonstrated that the results correlate to observed effects. The Europe-wide application of this method showed that 79% of sites were expected to have more than 5% of species affected due to chronic exposure, and 43% of sites were expected to have more than 5% of species affected due to peak exposure. Malaj et al. (2014) analysed measured concentration data from 4,000 European monitoring sites, compared these to species-specific toxicity data, and concluded that chronic effects were expected at 42% of sites, and acute lethal effects at 14% of sites. They observed that their results are likely to underestimate the actual risks, due to the limited number of chemicals measured. Lemm et al. (2020) analysed the correlation between the reported observed ecological status of European water bodies on one hand and multiple stressors expected to affect aquatic ecosystems on the other hand. For the toxic stress, the Posthuma et al. (2019) msPAF was used. Lemm et al. (2020) concluded that spatial variability of toxic stress was a significant explanatory factor for observed ecosystem status variability. Based on these assessments, the Posthuma et al. simulated msPAF is considered a realistic and credible metric of toxic stress.

The value of the HIWAI proxy as defined above was determined using the European-scale pollutant transport model by van Gils et al. (2020). Figure 3. 2 shows the correlation between the HIWAI (expressed as PP m^{-3}) and the effect metric (msPAF-EC50-P99) by Posthuma et al. (2019). There is a strong correlation between the two. There is obviously also variability not explained by the HIWAI, due to the information and processes not resolved. The two sides of the area covered by the cloud of points present two ways to link the expected toxic stress to the HIWAI. The red line in Figure 3. 2 represents the maximum expected effect level at a given HIWAI: the effects are not expected to exceed this level (the “worst case” option). The blue line represents a best case: the effects expressed by this line are the minimum that can be expected for a given HIWAI (the “best case” option). Areas that show effects according to this line can truly be considered to be hot spots.

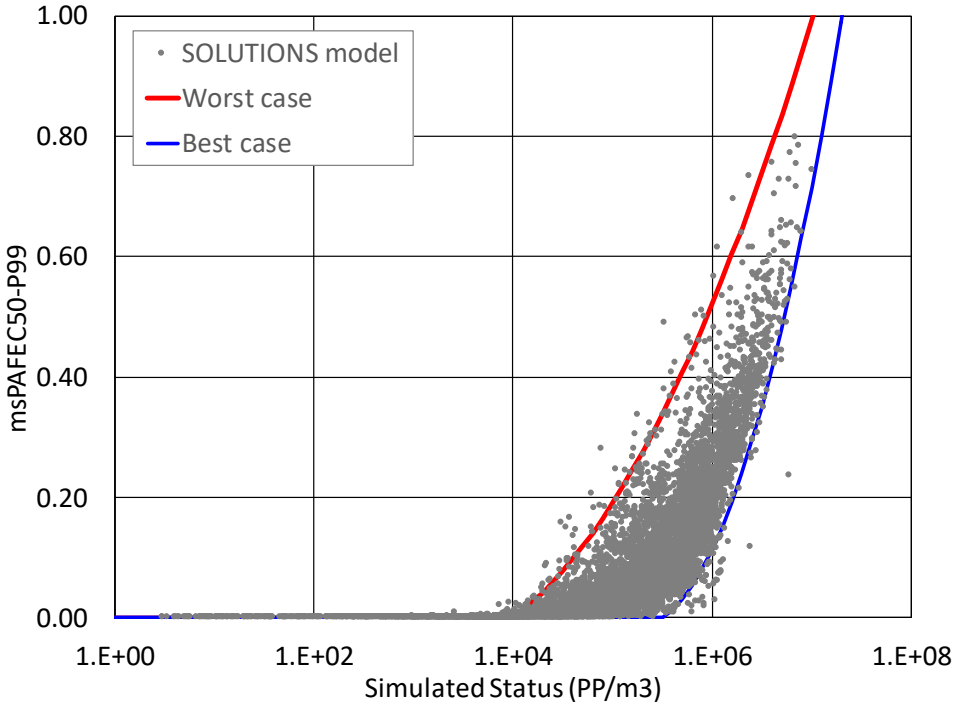

Figure 3. 2 Relation between HIWAI (x-axis, 'simulated status' expressed as PP m^{-3}) and ecological impact expressed by the msPAF-EC50-P99 metric (y-axis) as calculated by Posthuma et al. (2019) using predicted environmental concentrations of 1,785 chemicals by van Gils et al. (2020). The blue and red lines represent low ("best case" option) and high end ("worst case" option) ecological impact at a given HIWAI.

Using the blue and red lines in Figure 3. 2, two effect curves have been composed to link HIWAI to the expected toxic effects on aquatic species:

$$If\ log(HIWAI) > a\ then\ Impact = Min\ (\ b\ [log(HIWAI)-a] + c\ [log(HIWAI)-a]^2\ ,\ 1)$$

The coefficients *a, b* and *c* and the intersections with msPAF = 0.05-0.25-0.5-0.75 of the red and blue lines are listed in Table 3. 1.

Table 3. 1 Coefficients in effect curves linking HIWAI to ecological impact expressed by the msPAF-EC50-P99 metric as calculated by Posthuma et al. (2019) using predicted environmental concentrations of 1,785 chemicals by van Gils et al. (2020).

	worst case option	**best case option**
Coefficients	a = 4, b = 0.12, c = 0.07	a = 5.5, b = 0.1, c = 0.25
Status values for effect = 0.05– 0.25-0.50-0.75 resp.	22-166-895-3377 (x1000)	617-2094-5370-11110 (x1000)

Uncertainties

The method outlined here comes with relevant uncertainties. At the same time, it avoids certain uncertainties by stepping away from a substance-by substance modelling approach that would be highly uncertain, due to a lack of input data and model calibration data. Moreover, it relies on a few basic assumptions that have proven to be robust. The first assumption is that increasing stream dilution capacity leads to better water quality.

The second assumption is that the pollution pressure from human activities is concentrated in areas with high population density and productivity. These two assumptions are reflected in the name of the HIWAI proxy.
The relation between the HIWAI proxy and toxic stress to aquatic ecosystems has not yet been “ground-truthed” by showing that the HIWAI is correlated to observed toxic effects on ecosystems in the field. This relation has however been made plausible by correlating the HIWAI to simulated effects on ecosystems based on continental scale modelling of the concentrations of 1,785 chemicals. It can be argued that the collection of 1,785 modelled chemicals is still far from complete. The actual number of chemicals in aquatic ecosystems may be 1 or even 2 orders higher. At the same time, the fraction of sites showing toxic effects in these simulations was substantially higher than the fraction of sites expected to suffer from toxic effects based on measured chemicals concentrations. This is fully in line with expectations as the number of chemicals analysed in the field samples was much smaller than 1,785 at most sites. In addition, the spatial gradients of the simulated toxic pressure were demonstrated to explain a significant part of the spatial gradients of observed ecosystem status, next to other commonly identified stressors to aquatic ecosystems such as habitat destruction or eutrophication. At this stage of the scientific quest for a suitable method to assess the risks to ecosystems of the full mixture of man-made chemicals, more cannot yet be expected.

The choice was made to focus in this report on the “best case” correlation between the HIWAI and the toxic stress (blue line in Figure 3. 2). This line correlates HIWAI to a level of toxic stress that is the minimum expected (assuming that the methodology is correct). This is on one hand an optimistic approach, as the correlations presented here indicate that the level of toxic stress may very well be higher than what the blue line indicates. In view of the uncertainties associated to this method, a methodologically conservative approach was chosen, as not to suggest problems that may later turn out to be unrealistic. It is further noted that the choice for the blue line (and not the red line) only affects the predicted absolute level of stress. It does however not essentially affect the expected spatial gradients or the simulated time trends. An indication of the effects of the “worst case” correlation is also shown in this report (see Figure 3. 6).

The method used here relies on the correlation between the HIWAI and the simulated effects on ecosystems for the European continent. A relevant question is whether these results can be extrapolated to other continents:

- Is the proportionality between the chemicals use volume and GDP valid?
- Is the intrinsic toxicity of the chemicals used on other continents the same as in Europe?
- Is the relation between environmental management and control applied and the GDP that was used in Europe also valid outside Europe?
- Is the share of emissions avoided at maximum environmental management and control the same in other continents as in Europe?

This has not been systematically investigated yet. Some observations can be made, however. The assumption of proportionality between the chemicals use volume and GDP was supported by global data (see paragraph 3.2.2 ‘Why a proxy-based method?’). The relation between environmental management and control applied and the GDP was partly supported by global data, related to management of plastic waste (Lebreton et al. 2019). We see no immediate reason why the share of emissions avoided at maximum environmental management would be different outside Europe than inside Europe. There may be some concern related to the intrinsic toxicity of the chemicals used on other continents. In terms of regulating the admission of chemicals on the market, Europe can be considered a frontrunner, probably together with North America.

It cannot be excluded that chemicals prohibited for use in these continents because of their environmental effects, are exported to other continents. If this is the case, the chemicals used there may be more toxic than those used in Europe. The method used here could then present a too optimistic image for other continents than Europe and North America.

3.2.3 Input parameters

The input of the Delwaq simulation consists of hydrodynamics from the WFLOW simulation and two maps: a map of population density and a regionalized map of the gross domestic product based on purchasing power parity (GDP-PPP). These maps are both provided by PBL for the Baseline and the RCP6.0/SSP2 and RCP8.5/SSP5 scenarios. Both maps have a raster format with a grid size of 1/120 degrees. Around the equator this makes for a grid size of about 1 km by 1 km. Closer to the north and south pole the longitudinal resolution decreases due to the curvature of the earth while the latitudinal resolution remains the same. This results in a grid size of about 0.3 km by 1 km in northern Siberia.

3.2.4 Baseline and scenarios

To generate the Baseline results, hydrology calculations have been carried out for the years 1990-2020. Toxic stress calculations were done for a two-year period (2009 and 2010) and the average of the results for the year 2010 have been used to present in this report.

Two different scenarios have been simulated for future projections. The socio-economic pathway SSP2 (a middle of the road pathway or business-as-usual world) is combined with the RCP6.0 scenario and a more extreme combination of SSP5 (high growth of income, fossil fuel based) in combination with high global average radiative forcing values of the RCP8.5 scenario. Calculations for hydrology and toxic stress were made for the years 2049 and 2050. Toxic stress results for 2050 are shown in this report.

3.3 Results

3.3.1 Geographical scale

The Wflow simulation calculates for each raster cell the stream order. This stream order gives a number to each cell which is a measure of the importance of the cell in the drainage network. In the Wflow simulation a cell with a higher stream order has a higher importance in the drainage network. This stream order is independent of the amount of waterflow through the cells. For all figures and tables in this report the cells with a minimal stream order of 5 have been used. The cells with a stream order of 5 can be seen for instance in the Netherlands as the larger brooks with a regional drainage function.

The toxic stress model calculations are available on a detailed grid scale (1 km x 1 km at the equator) and may be used for regional analysis. The results can be aggregated easily to a higher level, such as country, river basin, global region or global scale (see Figure 3. 3).

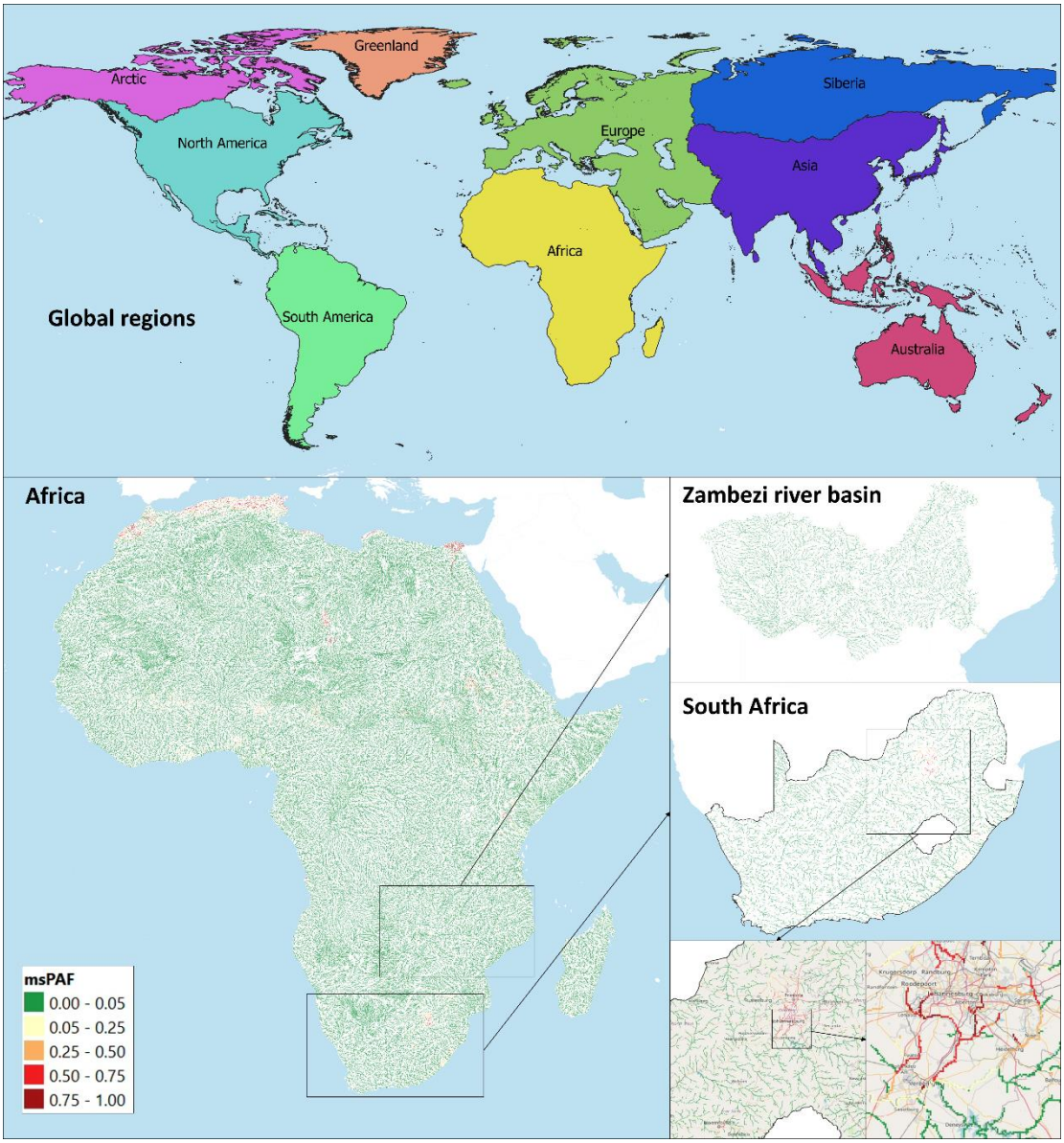

Figure 3. 3 Overview of the different scales for which the Toxic Stress calculation results can be presented: global scale and 9 distinguished global regions, global region (example Africa), river basin (example Zambesi river basin), country (example South Africa), regional and local scales (area around Johannesburg).

Figure 3. 4 shows the number of grid cells or the 9 global regions that are distinguished in this report.

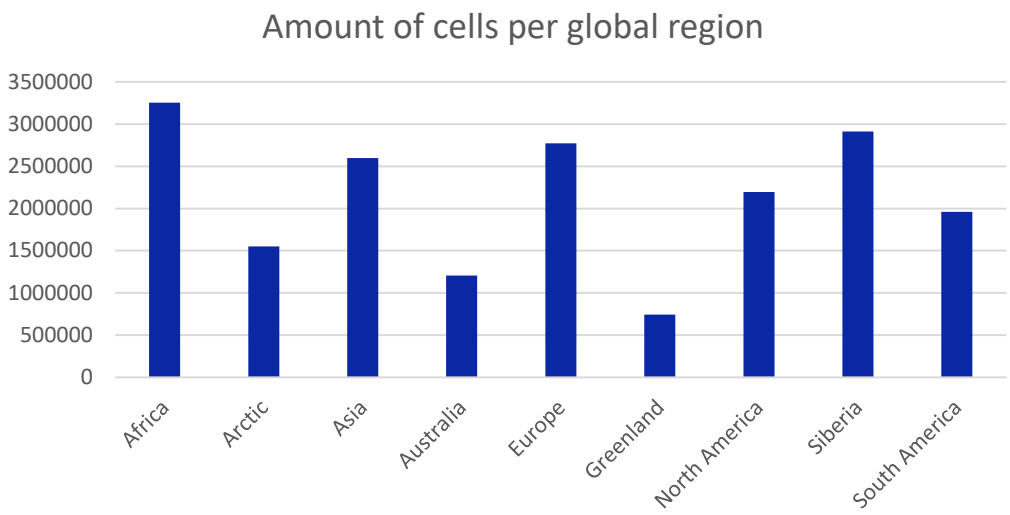

Figure 3. 4 The number of grid cells in the Toxic Stress calculation for the 9 distinguished global regions.

3.3.2 Sustainable Development Goals

The indicator for toxic stress can be related to the Sustainable Development Goals (SDGs). The percentage of grid cells with a msPAF <0.05 (meaning <5% of species are expected to be lost) is related in this report to the SDG Indicator 6.3.2 “Proportion of bodies of water with good ambient water quality”. So, the green areas on the maps represent water bodies with “a good water quality”.

3.3.3 Baseline

A global overview of the calculated msPAF as an indicator for the expected loss of aquatic species for the Baseline 2010 for the “best case” option is shown in Figure 3. 5A. On a global scale, 91% of the water bodies show a “good quality” (msPAF < 0.05) in the Baseline situation in 2010. Large differences can be seen between the different global regions (see Figure 3. 7): the lowest percentage of water bodies with a “good quality” are shown in Asia (76%), Europe (83%) and North America (84%). In the “worst case” option (see Figure 3. 6) the percentage of water bodies with a “good quality” on a global scale is much lower: 71%.

3.3.4 Scenarios

A global overview of the calculated toxic stress concerning the “best case” option for the RCP6.0/SSP2 2050 scenario and the RCP8.5/SSP5 2050 scenario is given in Figure 3. 5B and Figure 3. 5C. On a global scale, the percentage of water bodies with a “good quality” (msPAF < 0.05) show a decrease of 6% in the RCP6.0/SSP2 scenario and an even higher decrease of 8% in the RCP8.5/SSP5 scenario. The global maps of the ‘worst case’ calculations of the scenarios can be seen in Figure 3. 6. In the “worst case” option the percentage of water bodies with a “good quality” on a global scale declines to 62% in the RCP8.5/SSP5 scenario.

Figure 3. 7 shows the change of msPAF values in the grid cells for the Baseline and the two scenarios for the nine distinguished global regions for the “best case” option. Especially in Africa, Asia, Europe and North America a decrease of grid cells achieving good water quality (msPAF < 0.05) of about 13-14% can be observed. While the grid cells with high msPAF values (0.75 – 1) increase from the baseline to the RCP8.5/SSP5 scenario, specifically in Asia (ca. 10%), but also in Europe and North America (ca. 4%) and Africa (2%). The same trends, but with less percentage of grid cells changing, could be observed in Australia and South America. Minor to no changes in the scenarios were seen in the Arctic region, Greenland and Siberia, where msPAF values were mainly below 0.05.

Nevertheless, the trend for the whole world indicates that toxic pressure for aquatic species increases, which is demonstrated by an overall decrease (ca. 8%) of grid cells with lower msPAF values (< 0.05) in the baseline 2010 and an increase (ca. 3%) of high msPAF values (0.75 – 1) in the RCP8.5/SSP5 2050 scenario. These results illustrate that there are expected to be more hot spot areas in the future and further, that hot spot areas are getting larger and general toxicity increases in these regions. Some examples of hot spot areas can be seen in Figure 3. 8.

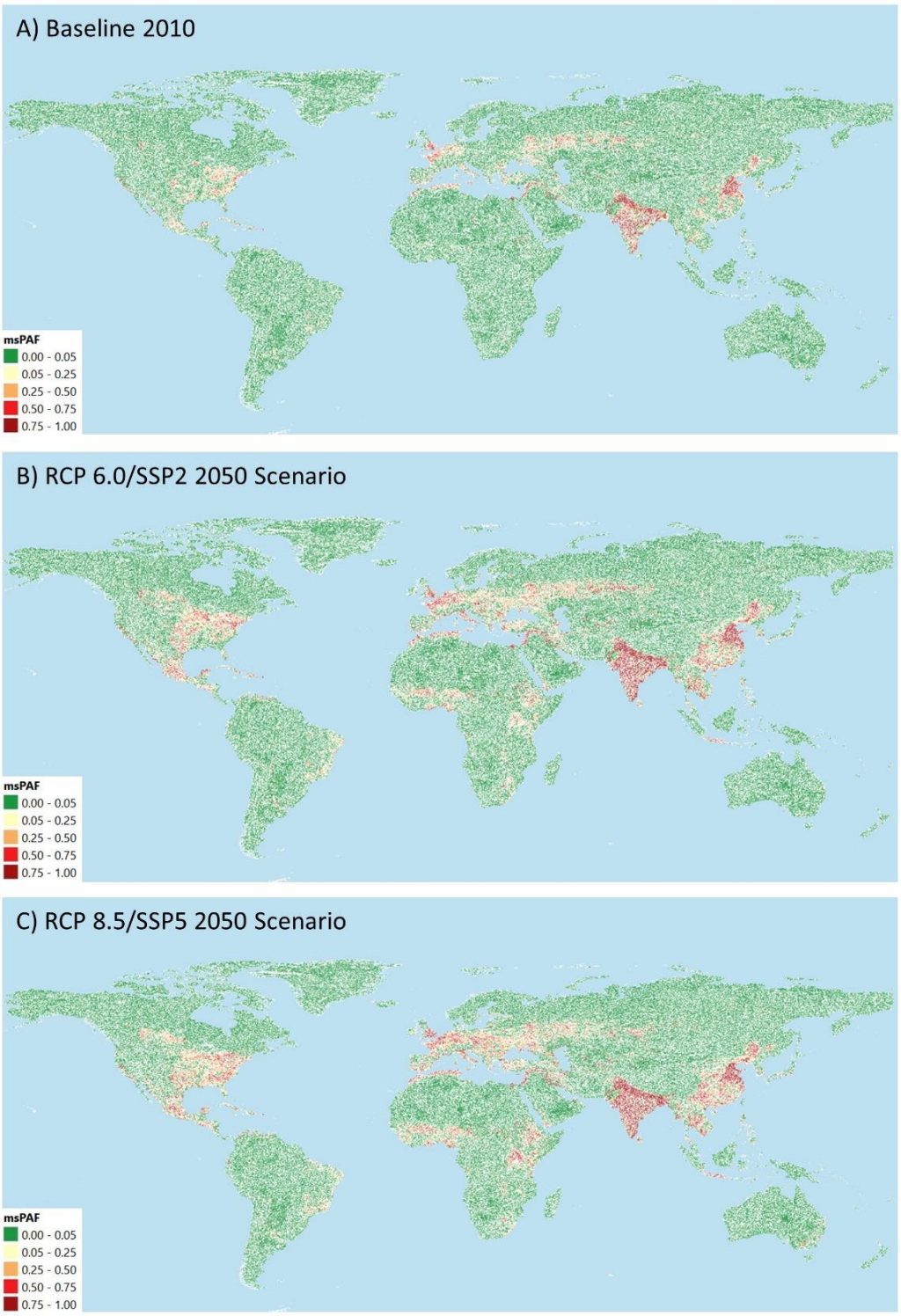

Figure 3. 5 Global maps of the "best case" option for the Baseline 2010 (A), RCP6.0/SSP2 2050 scenario (B) and RCP8.5/SSP5 2050 scenario (C) showing acute toxic pressure by chemicals, expressed in the terms of msPAF (multi-substance potentially affected fraction of species), indicating the expected species loss, ranging from 0 (no species affected) to 1 (all species affected).

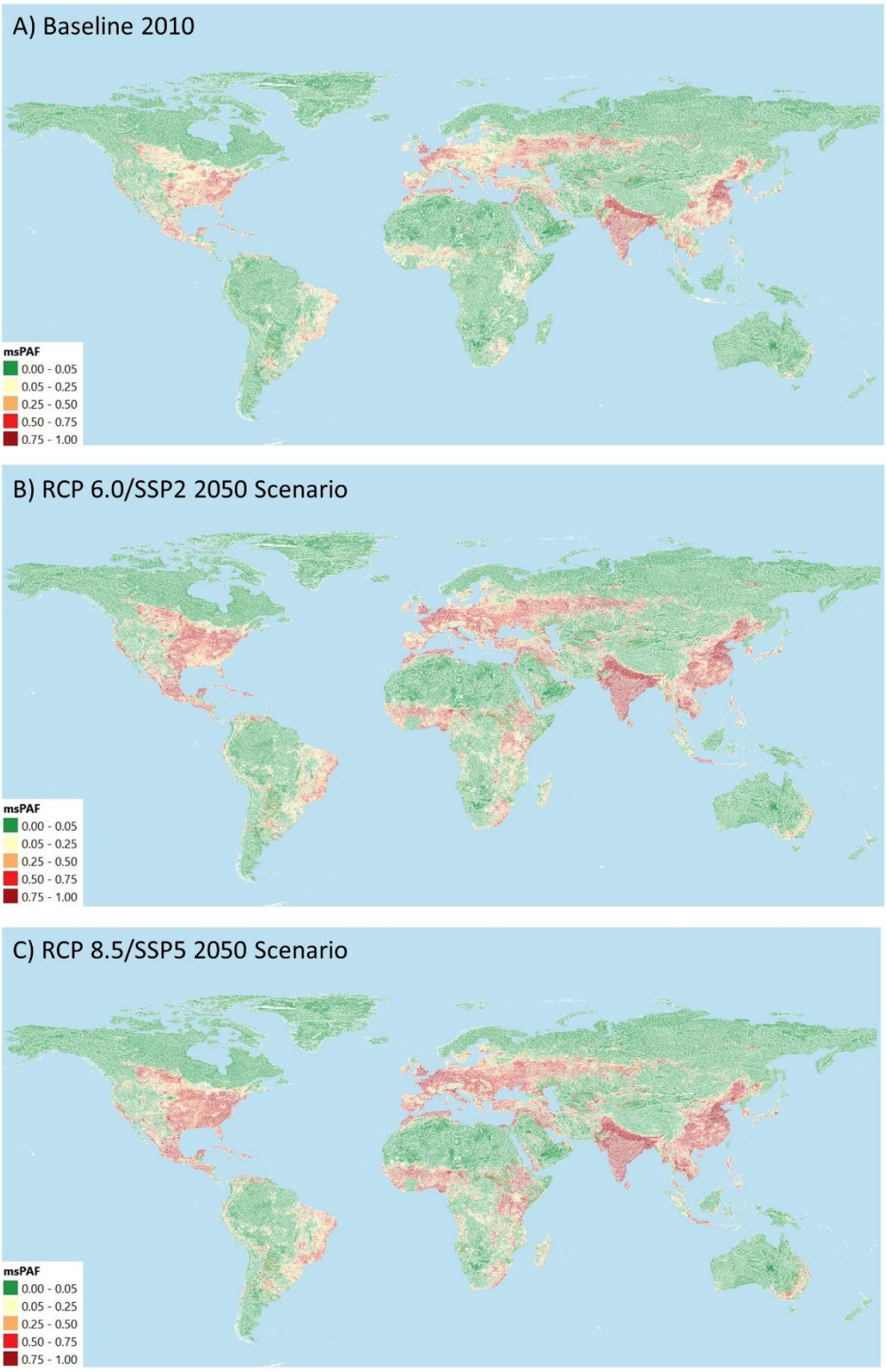

Figure 3. 6 Global maps of the "worst case" option for the Baseline 2010 (A), RCP6.0/SSP2 2050 scenario (B) and RCP8.5/SSP5 2050 scenario (C) showing acute toxic pressure by chemicals, expressed in the terms of msPAF (multi-substance potentially affected fraction of species), indicating the expected species loss, ranging from 0 (no species affected) to 1 (all species affected).

Figure 3. 7 "Best case" option results with percentage of grid cells showing acute toxicity expressed by msPAF (multi-substance potential affected fraction of species ranging from 0 (no species affected) to 1 (all species affected)) for the Baseline 2010 (blue), the RCP6.5/SSP2 2050 scenario (orange) and the RCP8.5/SSP5 2050 scenario (grey) for the whole world and for the 9 distinguished global areas.

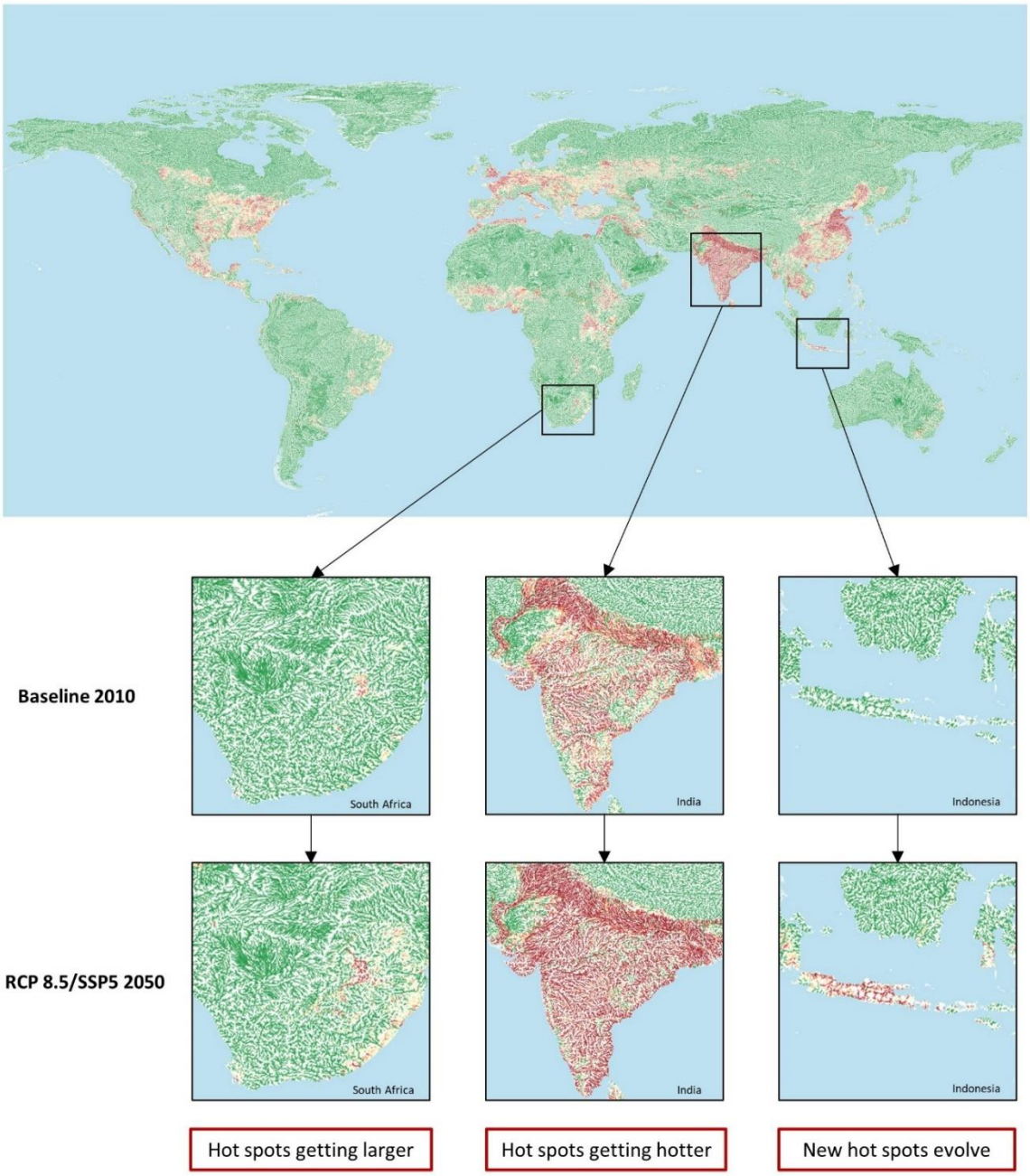

Figure 3. 8 "Best case" option examples of hot spot areas in global regions that get larger, increase in toxicity (getting hotter) and newly evolve in the RCP8.5/SSP5 2050 scenario in comparison to the Baseline 2010.

3.4 Conclusions

Based on the calculations of the Toxic Stress indicator, the following conclusions can be made:

- The Toxic Stress indicator for the expected loss of aquatic species can be linked to the SDG Indicator 6.3.2 “Proportion of bodies of water with good ambient water quality”. In this report a msPAF < 0.05 (meaning <5% of species are expected to be lost) is supposed to represent water bodies with “a good water quality”, shown on the maps as green areas.
- The Toxic Stress results are available on a detailed geographical scale (1 km x 1 km) and can be aggregated easily to large areas like river basins or countries, making it suitable for many purposes. In the Baseline situation in 2010 on a global scale 91% of the water bodies show a “good quality” (msPAF < 0.05) in the “best case” option, although large differences can be seen between the different global regions: the lowest percentage of water bodies with a “good quality” are shown in Asia (76%), Europe (83%) and North America (84%). Note that these results show the minimum impact to be expected and thus represent a best case. In the “worst case” option the percentage of water bodies with a “good quality” on a global scale is 71%.
- Two combinations of climate (RCP) and socioeconomic scenarios (SSP) are calculated for the year 2050. On a global scale, the percentage of water bodies with a “good quality” (msPAF < 0.05) show in the “best case” option a decrease of 6% in the RCP6.0/SSP2 scenario and an even higher decrease of 8% in the more extreme RCP8.5/SSP5 scenario. In the “worst case” option the percentage of water bodies with a “good quality” on a global scale in the RCP8.5/SSP5 scenario is 62%.
- Comparing the scenario calculations for 2050 with the Baseline situation in 2010, we see (both for the “best case” and the “worst case” option) a decrease of water bodies with “a good quality” and an increase of water bodies with a very high msPAF 0.8 – 1.0 in areas with already Toxic Stress problems. We see both “hot spots getting hotter”, “hot spots getting larger” and” more hot spots evolve” resulting in an overall increase of toxicity in these regions.
- The detailed calculation results will be made free available by the Deltares BlueEarth Digital Environment (https://blueearthdata.org/data).

4 References

American Chemistry Council (2019), Guide to the Business of Chemistry, https://www.americanchemistry.com/GBC2019.pdf; Figure 5.4 [accessed 28.04.2022]

Beusen, A., Bouwman, A., van Beek, L.P.H., Mogollon, J., and Middelburg, J.J. (2016). Global riverine N and P transport to ocean increased during the 20th century despite increased retention along the aquatic continuum. Biogeosciences 13(8), 2441-2451. doi: 10.5194/bg-13-2441-2016.

Beusen, A.H.W., Doelman, J.C., Van Beek, L.P.H., Van Puijenbroek, P.J.T.M., Mogollón, J.M., Van Grinsven, H.J.M., et al. (2022). Exploring river nitrogen and phosphorus loading and export to global coastal waters in the Shared Socio-economic pathways. Global Environmental Change 72, 102426. doi: https://doi.org/10.1016/j.gloenvcha.2021.102426.

Beusen, A.H.W., Van Beek, L.P.H., Bouwman, A.F., Mogollón, J.M., and Middelburg, J.J. (2015). Coupling global models for hydrology and nutrient loading to simulate nitrogen and phosphorus retention in surface water. Description of IMAGE-GNM and analysis of performance. Geoscientific Model Development 8, 4045–4067, doi:4010.5194/gmd-4048-4045-2015 (http://www.geosci-model-dev.net/4048/4045/2015/).

Bouwman, A.F., Beusen, A.H.W., Griffioen, J., Van Groenigen, J.W., Hefting, M.M., Oenema, O., et al. (2013). Global trends and uncertainties in terrestrial denitrification and N_2O emissions. Philosophical Transactions of the Royal Society B: Biological Sciences 368(1621). doi: 10.1098/rstb.2013.0112.

Brack, W., Valeria Dulio, Marlene Ågerstrand, Ian Allan, Rolf Altenburger, Markus Brinkmann, Dirk Bunke, Robert M. Burgess, Ian Cousins, Beate I. Escher, Félix J. Hernández, L. Mark Hewitt, Klára Hilscherová, Juliane Hollender, Henner Hollert, Robert Kase, Bernd Klauer, Claudia Lindim, David López Herráez, Cécil Miège, John Munthe, Simon O'Toole, Leo Posthuma, Heinz Rüdel, Ralf B. Schäfer, Manfred Sengl, Foppe Smedes, Dik van de Meent, Paul J. van den Brink, Jos van Gils, Annemarie P. van Wezel, A. Dick Vethaak, Etienne Vermeirssen, Peter C. von der Ohe, Branislav Vrana. (2017): Towards the review of the European Union Water Framework Directive: Recommendations for more efficient assessment and management of chemical contamination in European surface water resources. Science of The Total Environment, 576, 720-737, https://doi.org/10.1016/j.scitotenv.2016.10.104.

Damania, R., Desbureaux, S., Rodella, A.-S., Russ, J. and Zaveri, E. (2019). Quality Unknown: The Invisible Water Crisis. The World Bank. https://doi.org/10.1596/978-1-4648-1459-4.

Deltares (2022): Delft3D 4 - Open Source Community, https://oss.deltares.nl/web/delft3d [accessed 28.04.22]

Deltares (2021). Focus on the Future, Fast Forward Now. Strategic Agenda 2022-2025.

De Zwart, D., Posthuma, L., 2006. Complex mixture toxicity for single and multiple species: proposed methodologies. Environmental Toxicology and Chemistry 24, 2665-2672. DOI: 10.1897/04-639R.1.

Diaz, R.J. and Rosenberg, R. (2008). Spreading dead zones and consequences for marine ecosystems. Science 321, 926–929.

Doelman, J.C., Stehfest, E., Tabeau, A., van Meijl, H., Lassaletta, L., Gernaat, D.E.H.J., et al. (2018). Exploring SSP land-use dynamics using the IMAGE model: Regional and gridded scenarios of land-use change and land-based climate change mitigation. Global Environmental Change 48**,** 119-135. doi: 10.1016/j.gloenvcha.2017.11.014

Hempel, S., Frieler, K., Warszawski, L., Schewe, J., and Piontek, F. (2013). A trend-preserving bias correction – the ISI-MIP approach. Earth Syst. Dynam. 4(2)**,** 219-236. doi: 10.5194/esd-4-219-2013

ECHA (2022): Understanding REACH, https://echa.europa.eu/en/regulations/reach/understanding-reach [accessed 28.04.2022]

Hempel, S., Frieler, K., Warszawski, L., Schewe, J., and Piontek, F. (2013). A trend-preserving bias correction – the ISI-MIP approach. *Earth Syst. Dynam.* 4(2)**,** 219-236. doi: 10.5194/esd-4-219-2013.

Howarth, R., Chan, F., Conley, D.J., Garnier, J., Doney, S.C., Marino, R. and Billen, G. (2011). Coupled biogeochemical cycles: Eutrophication and hypoxia in temperate estuaries and coastal marine ecosystems. Frontiers in Ecology and the Environment 9(1), 18–26. https://doi.org/10.1890/100008

Klein Goldewijk, K., Beusen, A., and Janssen, P. (2010). Long-term dynamic modeling of global population and built-up area in a spatially explicit way: HYDE 3.1. Holocene 20(4)**,** 565-573.

Lebreton, L., Andrady, A. Future scenarios of global plastic waste generation and disposal. Palgrave Commun 5, 6 (2019). https://doi.org/10.1057/s41599-018-0212-7, Figure 1B

Lemm, Jan; Venohr, Markus; Globevnik, Lidija; Stefanidis, Konstantinos; Panagopoulos, Yiannis; van Gils, Jos; Posthuma, Leo; Kristensen, Peter; Feld, Christian; Mahnkopf, Judith; Hering, Daniel; Birk, Sebastian. Multiple stressors determine river ecological status at the European scale: Towards an integrated understanding of river status deterioration. Global Change Biology, https://doi.org/10.1111/gcb.15504.

Liska, I., Wagner, F., Sengl, M., Deutsch, K. and Slobodnik, J. (2015). Joint Danube Survey 3 A Comprehensive Analysis of Danube Water Quality. ICPDR – International Commission for the Protection of the Danube River. Vienna/Austria. Retrieved from http://www.danubesurvey.org/sites/danubesurvey.org/files/nodes/documents/jds3_final_scientific_report _1.pdf.

MetOffice (2020). HadCM3: Met Office climate prediction model. https://www.metoffice.gov.uk/research/approach/modelling-systems/unified-model/climate-models/hadcm3.

Newbold, J.D., Elwood, J.W., O'Neill, R.V., and Winkle, W.V. (1981). Measuring nutrient spiraling in streams. Canadian Journal of Fisheries and Aquatic Sciences 38**,** 860-863.

Malaj, E., von der Ohe, P., Grote, M., Kühne, R., Mondy, C., Usseglio-Polatera, P., et al., 2014. Organic chemicals jeopardise freshwater ecosystems health on the continental scale. Proc. Natl. Acad. Sci. 111, 9549–9554. DOI: 10.1073/pnas.1321082111.

Michalak, A.M., Anderson, E.J., Beletsky, D., Boland, S., Bosch, N.S.m Bridgeman, T.B. et al. (2013). Recordsetting algal bloom in Lake Erie caused by agricultural and meteorological trends consistent with expected future conditions. Proceedings of the National Academy of Sciences 110(16), 6448–6452. https://doi.org/10.1073/pnas.1216006110

O'Neill, B.C., Kriegler, E., Riahi, K., Ebi, K.L., Hallegatte, S., Carter, T.R., et al. (2014). A new scenario framework for climate change research: the concept of shared socioeconomic pathways. Climatic Change 122(3)**,** 387-400. doi: 10.1007/s10584-013-0905-2.

Posthuma, L., van Gils, J., Zijp, M. C., van de Meent, D., & de Zwart, D. (2019). Species sensitivity distributions for use in environmental protection, assessment, and management of aquatic ecosystems for 12 386 chemicals. Environmental Toxicology and Chemistry, 38(4), 703–711. https://doi.org/10.1002/etc.4373.

Rabalais, N.N., Turner, R.E. and Wiseman, W.J. (2001). Hypoxia in the Gulf of Mexico. Journal of Environmental Quality 30(2), 320–329.

Schulze, S., Zahn, D., Montes, R., Rodil, R., Benito Quintana, J., Knepper, T., et al. (2019). Occurrence of emerging persistent and mobile organic contaminants in European water samples. Water Res 153, 80–90. https://doi.org/10.1016/j.watres.2019.01.008.

Stehfest, E., Van Vuuren, D.P., Kram, T., and Bouwman, A.F. (2014). Integrated Assessment of Global Environmental Change with IMAGE 3.0. Model description and policy applications. The Hague: PBL Netherlands Environmental Assessment Agency (http://themasites.pbl.nl/models/image/index.php/Main_Page).

Stroomberg, G., Neefjes, R., Jonge, J., Bannink, A., Haar, G. and Zwamborn, C. (2018). Jaarrapport 2017, De Rijn. RIWA-Rijn. Nieuwegein, The Netherlands. Retrieved from https://www.riwa-rijn.org/publicatie/jaarrapport2017-de-rijn/.

Sutanudjaja, E.H., Van Beek, R., Wanders, N., Wada, Y., Bosmans, J.H.C., Drost, N., et al. (2018). PCR-GLOBWB 2: A 5 arcmin global hydrological and water resources model. Geoscientific Model Development 11(6), 2429-2453. doi: 10.5194/gmd-11-2429-2018.

Turner, R.E., Rabalais, N.N., Justic, D. and Dortch, Q. (2003). Global patterns of dissolved N, P and Si in large rivers. Biogeochemistry, 64, 297–317.

UN (2015). Resolution adopted by the General Assembly on 25 September 2015: 70/1. Transforming our world: the 2030 Agenda for Sustainable Development.

UNEP (2016). A Snapshot of the World's Water Quality: Towards a Global Assessment. United Nations Environment Programme, Nairobi, Kenya. 162pp.

UNEP (2018). Resolution 3/10 on "Addressing water pollution to protect and restore water-related ecosystems" (UNEP/EA.3/Res.10). https://wedocs.unep.org/bitstream/handle/20.500.11822/27177/Implementation%20of%20UNEA%20resolution%203-10%20.pdf?sequence=6&isAllowed=y

UNESCO and HELCOM (2017). Pharmaceuticals in the Aquatic Environment of the Baltic Sea Region — A Status Report. Paris: UNESCO Publishing.

UN-Water (2016). Towards a Worldwide Assessment of Freshwater Quality. A UN-Water Analytical Brief. UN-Water, Genève, Switzerland. 36pp.

Van Beek, L.P.H., Wada, Y., and Bierkens, M.F.P. (2011). Global monthly water stress: 1. Water balance and water availability. Water Resour. Res. 47(7), W07517. doi: 10.1029/2010wr009791.

Van Drecht, G., Bouwman, A.F., Knoop, J.M., Beusen, A.H.W., and Meinardi, C.R. (2003). Global modeling of the fate of nitrogen from point and nonpoint sources in soils, groundwater and surface water. Global Biogeochemical Cycles 17, 1115, doi:10.1029/2003GB002060.

van Gils, J., Posthuma, L., Cousins, I.T. et al. The European Collaborative Project SOLUTIONS developed models to provide diagnostic and prognostic capacity and fill data gaps for chemicals of emerging concern. Environ Sci Eur 31, 72 (2019). https://doi.org/10.1186/s12302-019-0248-3.

van Gils, J., Posthuma, L., Cousins, I. T., Brack, W., Altenburger, R., Baveco, H., … van Wezel, A. (2020). Computational material flow analysis for thousands of chemicals of emerging concern in European waters. Journal of Hazardous Materials, 397(April), 122655. https://doi.org/10.1016/j.jhazmat.2020.122655.

Van Puijenbroek, P.J.T.M., Beusen, A.H.W., and Bouwman, A.F. (2019). Global nitrogen and phosphorus in urban waste water based on the Shared Socio-economic pathways. *Journal of Environmental Management* 231, 446-456. doi: 10.1016/j.jenvman.2018.10.048.

van Vuuren, D.P., Kriegler, E., O'Neill, B.C., Ebi, K.L., Riahi, K., Carter, T.R., et al. (2014). A new scenario framework for Climate Change Research: scenario matrix architecture. Climatic Change 122(3), 373-386. doi: 10.1007/s10584-013-0906-1.

van Vuuren, D.P., Stehfest, E., Gernaat, D.E.H.J., Doelman, J.C., van den Berg, M., Harmsen, M., et al. (2017). Energy, land-use and greenhouse gas emissions trajectories under a green growth paradigm. Global Environmental Change 42, 237-250. doi: 10.1016/j.gloenvcha.2016.05.008.

Vollenweider, R.A. (1992). Coastal marine eutrophication: principles and control. Science of the Total Environment (Vol. Supplement, 1-20). https://doi.org/10.1016/B978-0-444-89990-3.50011-0

Wang, Z., Walker, G.W., Muir, D.C.G. and Nagatani-Yoshida, K. (2020). Toward a global understanding of chemical pollution: a first comprehensive analysis of national and regional chemical inventories. Environ. Sci. Technol. 54, 5, 2575-2584. https://doi.org/10.1021/acs.est.9b06379

Wollheim, W., Vörösmarty, C.J., Bouwman, A.F., Green, P., Harrison, J., Meybeck, M., et al. (2008). Global N removal by freshwater aquatic systems using a spatially distributed, within-basin approach. Global Biogeochemical Cycles 22, GB2026, doi:10.1029/2007GB002963.

World Bank (2022), International Comparison Program, World Bank | World Development Indicators database, World Bank | Eurostat-OECD PPP Programme, https://data.worldbank.org/indicator/NY.GDP.MKTP.PP.KD [accessed 28.04.2022]

World Water Quality Alliance (2021). World Water Quality Assessment: First Global Display of a Water Quality Baseline. A consortium effort by the World Water Quality Alliance - towards a full global assessment. Information Document Annex for display at the 5th Session of the United Nations Environment Assembly, Nairobi 2021.

Deltares is an independent institute for applied research in the field of water and subsurface. Throughout the world, we work on smart solutions for people, environment and society.

Deltares

www.deltares.nl